Copper-gold±silver mineralization at the Stu occurrence, central Yukon (Yukon MINFILE 115I011)

P.J. Sack[1] and S. Casselman
Yukon Geological Survey

D. James
Consultant, Duncan, British Columbia

B. Harris
Midnight Mining Services Ltd.

Sack, P.J., Casselman, S., James, D. and Harris, B., 2016. Copper-gold±silver mineralization at the Stu occurrence, central Yukon (Yukon MINFILE 115I011). *In:* Yukon Exploration and Geology, K.E. MacFarlane and M.G. Nordling (eds.), Yukon Geological Survey, p. 207-222, plus digital appendices.

ABSTRACT

The Stu copper-gold±silver occurrence (Yukon MINFILE 115I 011) is located midway between the Minto and Carmacks Copper deposits in the eastern, Minto suite portion of the Granite Mountain batholith. The best known mineralization at Stu is in Zone A, where at least four foliated and mineralized bodies strike northwest and dip moderately to steeply to the northeast. These bodies grade 0.2 to 0.6% total Cu, though the best historic diamond drill intersection contains 3.5% Cu over 13.5 m. In plan and cross section view, the foliated and mineralized granodioritic orthogneiss bodies pinch and swell, appearing as lenses surrounded by unfoliated K-feldspar porphyritic granodiorite. Copper mineralization occurs as both fine-grained hypogene bornite and chalcopyrite, and supergene malachite, azurite, tenorite and chrysocolla. This study suggests that Stu mineralization is similar to that at the Carmacks Copper and Minto deposits as it is primarily hosted in multiple, discrete bodies of foliated granodioritic rock. In terms of ore body orientation, the moderate to steeply dipping nature at Stu is more reminiscent of Carmacks Copper than Minto, which likely explains the presence of significant supergene copper mineralization.

[1]*patrick.sack@gov.yk.ca*

INTRODUCTION

In 2014, the Yukon Geological Survey (YGS) initiated a multi-year project investigating Late Triassic to Jurassic plutonic rocks in Yukon with the aim of providing an updated metallogenic framework for associated deposits and occurrences; the most significant of these are the Minto (Yukon MINFILE 115I021) and Carmacks Copper (Yukon MINFILE 115I008) deposits. The Stu copper-gold±silver occurrence (Yukon MINFILE 115I011) is another significant, albeit poorly documented, occurrence located 10 km northwest of the Carmacks Copper deposit (oxide resource of 12 Mt grading 0.9% oxide Cu (1.07% total Cu), 0.5 g/t Au and 4.6 g/t Ag; Arseneau and Casselman, 2008) and 30 km southeast of the Minto mine (sulphide resource 70.8 Mt grading 1.2 % Cu, 0.5 g.t Au and 4.2 g/t Ag; recalculated from Mercer and Sagman, 2012).

Historic mapping, soil sampling, bull dozer trenching, diamond drilling and rotary air-blast (RAB) drilling were done on the Stu property between 1971 and 1989. With the notable exception of assay data, a reasonable amount of this information is in the public realm, mostly as assessment reports. However, a synthesis of existing data has not been done, and the occurrence has only received cursory research during studies focused on the Minto and Carmacks Copper deposits (*e.g.*, Tafti and Mortensen, 2004). Work at the Stu occurrence conducted in 2015 by YGS staff, in collaboration with Bill Harris the property owner, was done over a five day period. Core from three key, historic diamond drill holes was re-logged and resampled, two re-excavated trenches mapped and four re-excavated trenches sampled. Thirteen representative samples have been analyzed for whole-rock geochemistry, and twenty samples from diamond drill hole 80-6 have been re-assayed for sulphide and supergene Cu mineralization. Historic drill hole and trench geology has been digitized and combined with the new data to create an updated geologic model for the occurrence. In the present contribution, we document and characterize mineralization at the Stu occurrence so that it can be placed into the larger metallogenic framework being developed for Late Triassic to Jurassic plutonic rocks in Yukon.

REGIONAL GEOLOGY

Accretion of the Intermontane terranes (Yukon-Tanana, Stikinia, Quesnellia and Cache Creek) to the western margin of North America in the Late Triassic to Jurassic resulted in prolific arc magmatism throughout the northern Cordillera (Nelson *et al.*, 2013). This period of magmatism is particularly important metallogenically as it hosts many of the porphyry copper (±Au, Mo) deposits in British Columbia (Logan and Mihalynuk, 2014). Locally, rocks of this age host the enigmatic Minto and Carmacks Copper deposits, as well as the Stu occurrence (Tafti and Mortensen, 2004). New geochronological, geochemical and petrographic evidence collected during the YGS's Late Triassic to Jurassic plutons project will result in reinterpretation of the magmatic suites of this age range in Yukon. These suites will be described in detail in other publications (*e.g.* Joyce *et al.*, 2016), but updated terminology will used in this paper. In Yukon, Late Triassic to Jurassic plutonic rocks can be divided into four magmatic suites, from oldest to youngest these are: Late Triassic Stikine Suite, latest Triassic to Early Jurassic Minto suite, Early Jurassic Long Lake Suite, and Middle Jurassic Bennett-Bryde suite (Fig. 1; following subdivisions of Woodsworth *et al.*, 1991; Gordey and Makepeace, 2001 and Colpron *et al.*, 2016).

The Stu occurrence is hosted within the Granite Mountain batholith which intrudes Yukon-Tanana terrane rocks along its southwest margin, and is faulted against Stikinia rocks to the northeast along the Hoocheekoo fault (Fig. 1). To the northwest, the batholith is overlain by mafic to intermediate volcanic rocks of the Carmacks Group and to the southeast, the Miller fault juxtaposes Carmacks Group volcanic rocks against the batholith (Tempelman-Kluit, 1984). Broadly, the batholith is composed of a western Long Lake suite part and an eastern Minto suite part (Fig. 1); the contact between the two is poorly understood, and may be associated with a fault. The Granite Mountain batholith is intruded by dacite dikes related to the Early Cretaceous Mt. Nansen Group volcanic rocks, and by mafic feeder dikes of the overlying Late Cretaceous Carmacks Group volcanic rocks (Tempelman-Kluit, 1984).

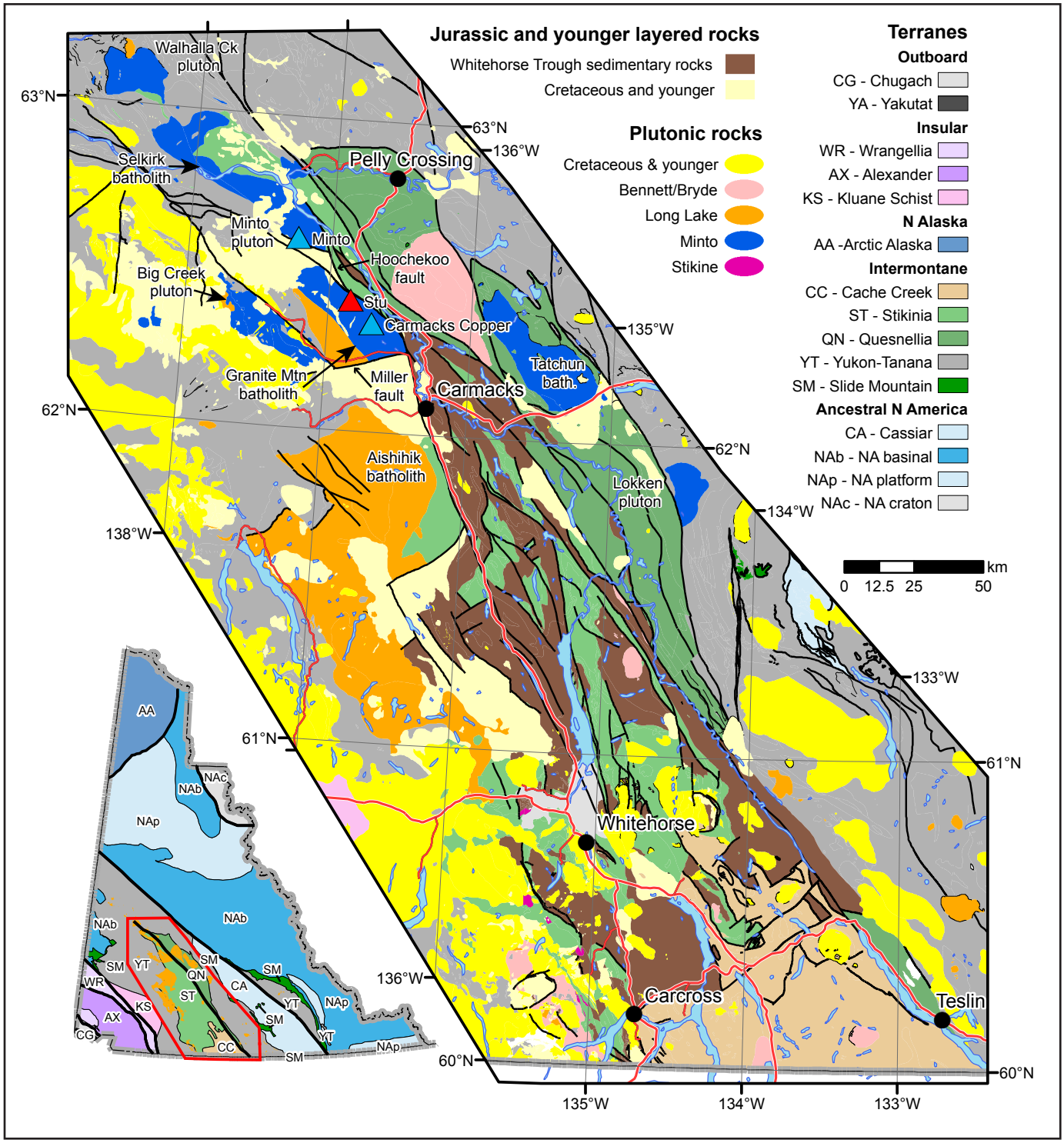

Figure 1. *Simplified geology of south central Yukon with emphasis on Late Triassic to Jurassic plutonic suites as described in text. Significant Early Jurassic Cu-gold±silver mineral occurrences shown by triangles, Stu in red. Inset, Yukon terrane map, area outlined in red shows the area of the main map. Geological data from Yukon Geological Survey (2015).*

PROPERTY GEOLOGY

Two main lithologies of plutonic rocks are recognized on the Stu property; for the purposes of the present paper we use the modal mineralogy QAP based classification of Le Bas and Streckeisen (1991). The southwestern margin of the property is underlain by a poorly understood equigranular quartz monzonitic rock while the majority of the property is underlain by variably foliated, fine to medium-grained, equigranular to K-feldspar porphyritic granodioritic rocks (Fig. 2). Geology and geophysical anomalies generally trend NW with the boundary between the quartz monzonitic rock and granodioritic rocks occurring in the transition between a relative magnetic low, to the southwest, and high to the northeast (Fig. 2 inset). Outcrop magnetic susceptibility

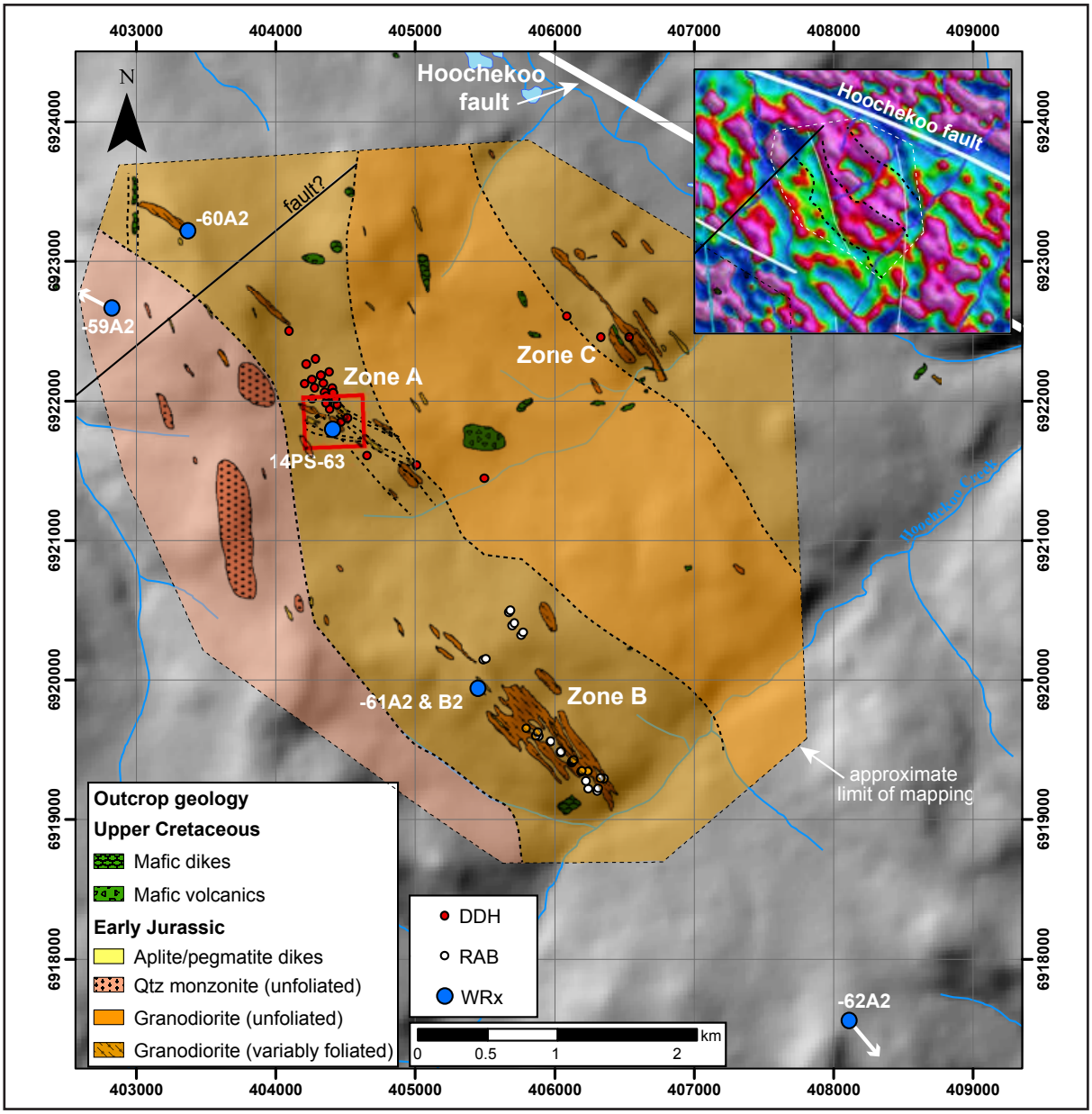

Figure 2. *Property outcrop map modified from Watson and Joy (1977); interpreted geology, in subdued colours, from the present study. Location of Figure 3 shown by red square. Samples -59A2 and -62A2 are approximately 4 and 1 km, respectively, off the map in the directions indicated by white arrow; coordinates for all samples are included in the digital appendices. Grid is UTM Zone 8, NAD83. Top right inset is the first vertical derivative of the enhanced magnetic field map from Hayward et al. (2012) and interpreted lineaments, in white, are from Sánchez et al. (2014). DDH=diamond drill hole collar, RAB=rotary air blast hole collar, WRx=whole-rock sample.*

measured at 63 stations throughout the Minto suite part of the Granite Mountain batholith average 4.13 x 10^3 SI units and range from 0.04 to 19.7. Supergene copper mineralization appears to be a relative magnetic low feature, likely due to oxidation effects on magnetite (Pautler, 2009).

The majority of bedrock exposed in trenches 600W and 800W (Fig. 3), and in diamond drill holes 80-6 (Fig. 4), 80-7 (Fig. 5), and 80-14, is weakly foliated to unfoliated K-feldspar porphyritic granodiorite. Within the porphyritic granodiorite are a series of strongly foliated bodies with a NW foliation dipping ~75° to the NE (Fig. 3). The bodies themselves appear to have a slightly shallower dip, between 40° and 70°, to the NE (Fig. 6; appendix 1). The degree of deformation and recrystallization of these rocks varies between unfoliated granodiorite, biotite schist and biotite orthogneiss (Figs. 4 and 5); with orthogneiss being more common than schist. Contacts between the three rock types are ambiguous. They generally transition over several cm, and locally K-feldspar phenocrysts in unfoliated

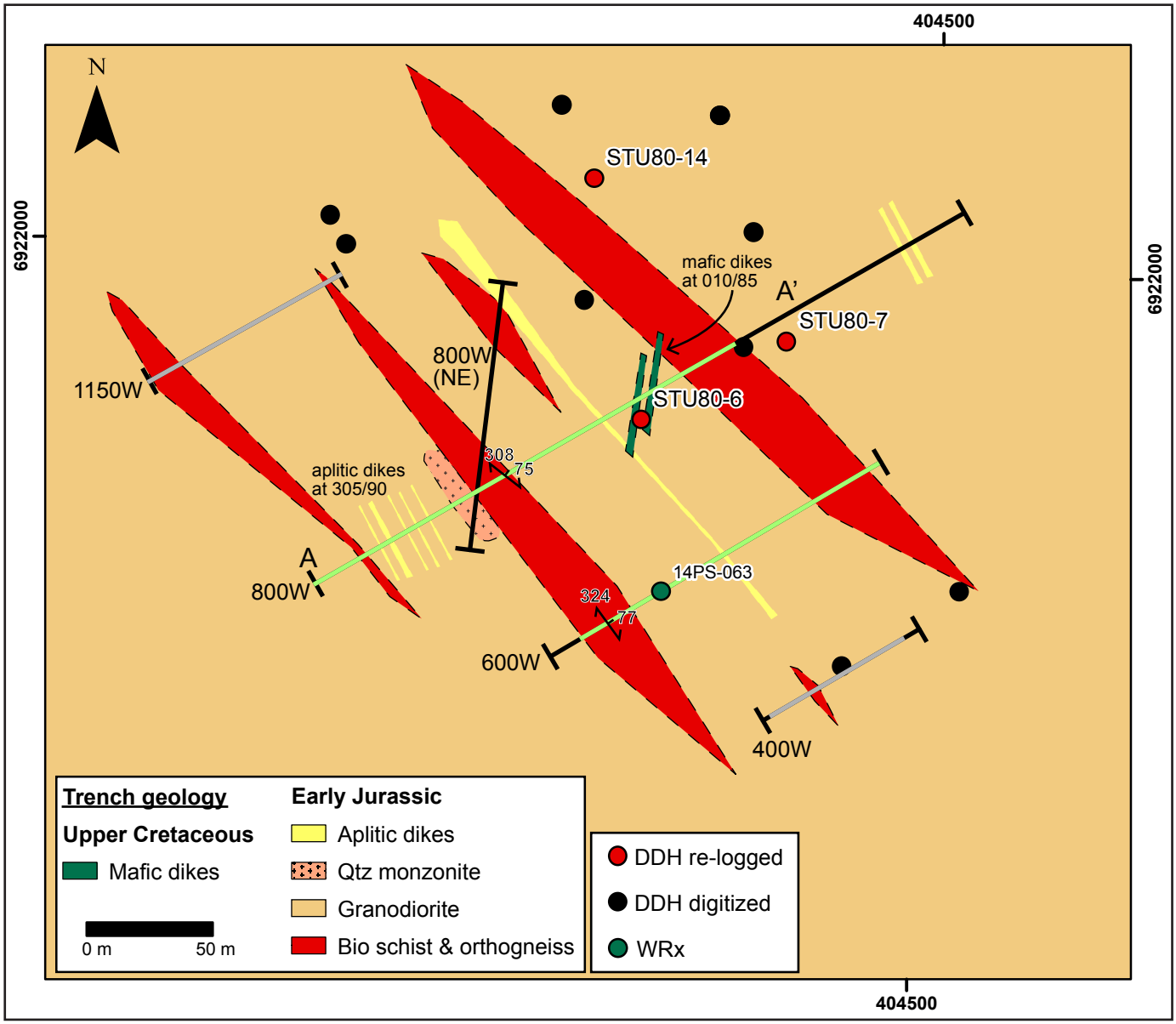

Figure 3. *Geologic sketch map of Zone A, based on 2015 trench mapping and reinterpretation of original trench mapping. Original 1978-79 trenches shown in black lines, parts of trenches shown in green were re-excavated, re-mapped and resampled in 2015, those in grey were not re-mapped but were resampled. Foliated and mineralized schist and gneiss shown in red is projected vertically to surface where not intersected by trenching. Cross section 800W in Figure 6 is A-A'. Bio = biotite, DDH = diamond drill hole, Qtz = quartz.*

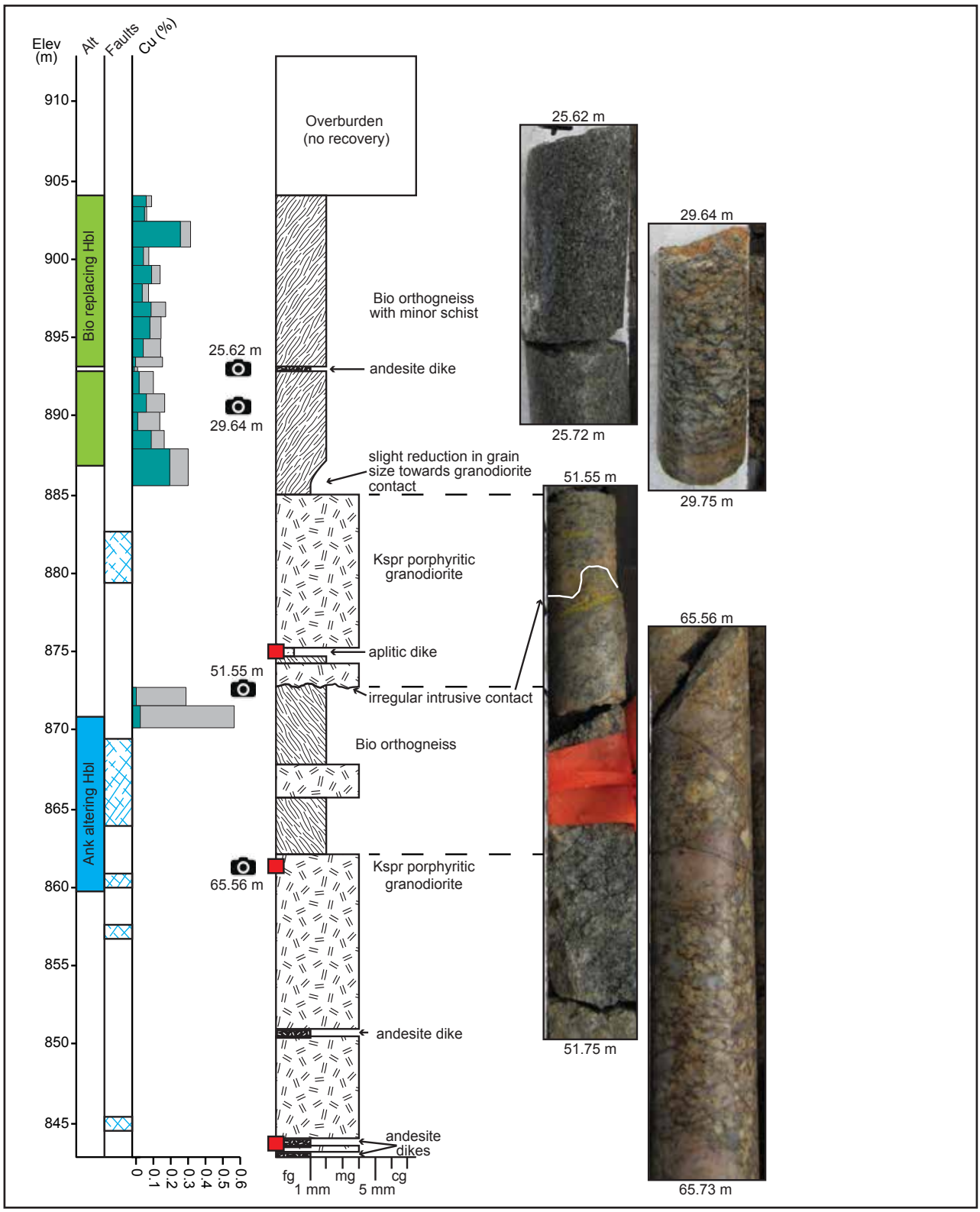

Figure 4. *Graphic log of diamond drill hole 80-6 re-logged and re-assayed in 2015 for the present study. Collar location shown on Figure 3. Pictures on right include from-to depths, above and below, respectively; all core is 3.65 cm diameter BQ size. Red squares show depths of 2015 samples. Alt = alteration; Cu = copper, reported as percentage of total Cu (grey) and supergene Cu (teal). Hbl = hornblende, Bio = biotite, Qtz = quartz, kspr = K-feldspar, Ank = ankerite, fg = fine-grained, mg = medium-grained, cg = coarse-grained.*

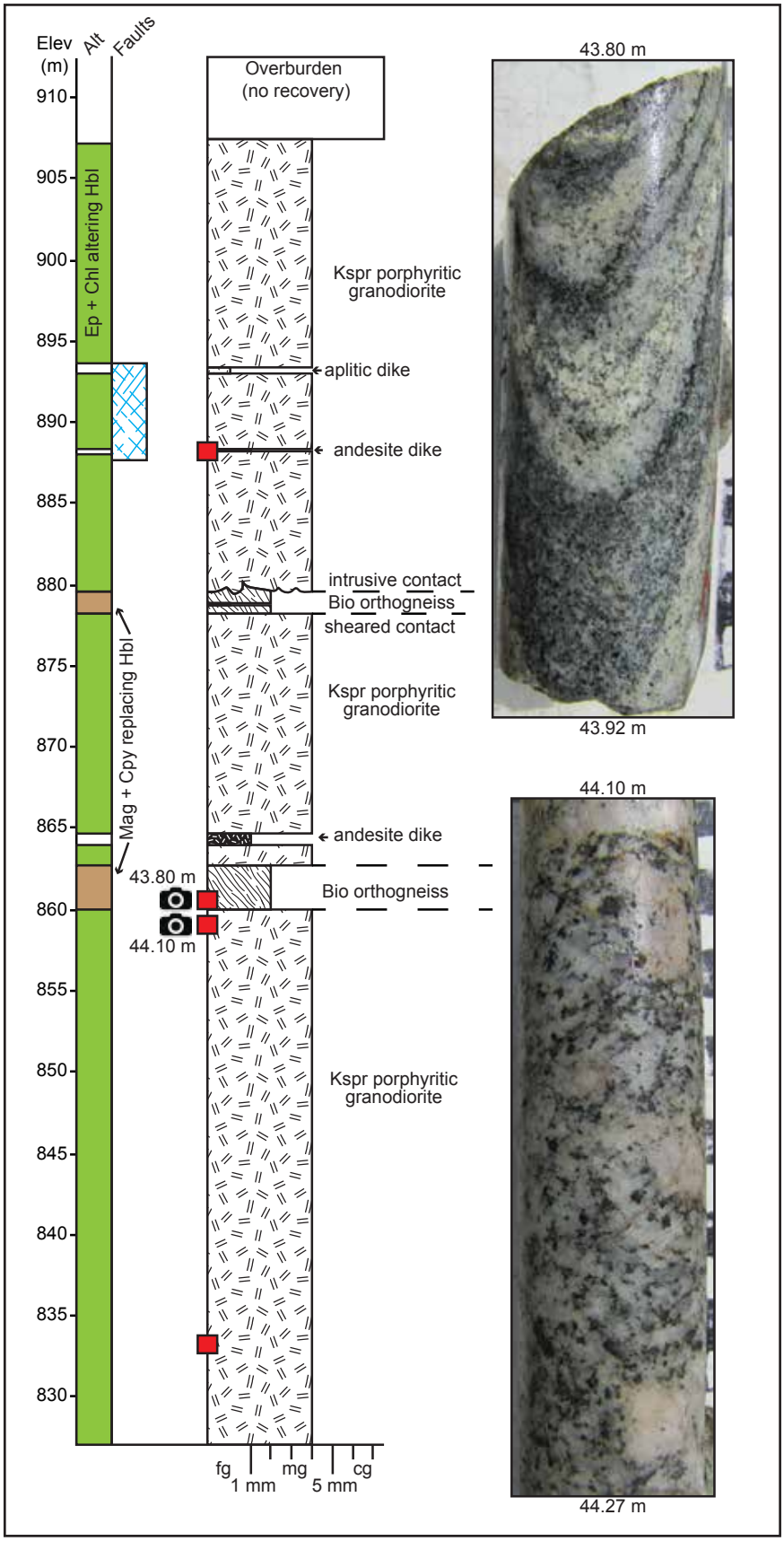

Figure 5. *Graphic log of drill hole 80-7 re-logged in 2015 for the present study, but not re-assayed. Collar location shown on Figure 3. Pictures on right shown include from-to depths above and below respectively; all core is 3.65 cm diameter BQ size. Ep=epidote, Mag=magnetite, Chl=chlorite, Cpy=chalcopyrite, other abbreviations and symbols same as Figure 4.*

granodiorite impinge foliated rocks suggesting that the contact is primarily intrusive. This coupled with overall rock distribution (Fig. 6) suggests that the unfoliated granodiorite engulfed earlier foliated varieties. Copper mineralization occurs as both supergene and sulphide minerals depending on level of oxidation (Fig. 6). Copper (Au ± Ag) mineralization is mostly associated with biotite schist and orthogneiss, though locally supergene copper minerals are found in unfoliated granodiorite.

Other intrusive rock types recognized locally, but not represented at the property map-scale include aplite and pegmatite dikes, microdiorite and andesite dikes. Small outcrops of Carmacks Group mafic volcanic rocks are found on the hilltops between Zone A and C (Fig. 2). Swarms of aplite and pegmatite dikes <1 m thick are generally steeply dipping with a NW strike. These dikes are found proximal to contacts between foliated and unfoliated varieties of granodiorite suggesting these contacts are zones of weakness. The aplite and pegmatite dikes are mineralogically and compositionally similar to the quartz monzonitic rocks, and are interpreted as late stage Early Jurassic intrusions related to the cooling of the Granite Mountain batholith. Based on crosscutting relationships, the interpreted intrusive sequence from oldest to youngest is: granodioritic orthogneiss – unfoliated granodiorite – quartz monzonite – aplite/pegmatite – microdiorite – andesite dikes (*e.g.*, Fig. 7).

PETROGRAPHY

Unmineralized massive porphyritic samples have a medium-grained groundmass of embayed and anhedral to subhedral felsic minerals (quartz, plagioclase and K-feldspar) with subhedral to euhedral randomly oriented mafic minerals (biotite and hornblende). Accessory titanite, magnetite and magmatic epidote are also present. Magmatic epidote is of particular interest as it has been used as petrographic evidence of a relatively deep emplacement depth for the plutons (>25 km crustal depth; Zen and Hammarstrom, 1984). Potassium feldspar phenocrysts are 1 to 3 cm long and are also randomly oriented. Groundmass plagioclase and K-feldspar (groundmass and phenocrysts) are moderately saussauritized. Quartz, plagioclase and hornblende all occur as inclusions within K-feldspar phenocrysts. The unfoliated granodiorite is generally unaltered to weakly

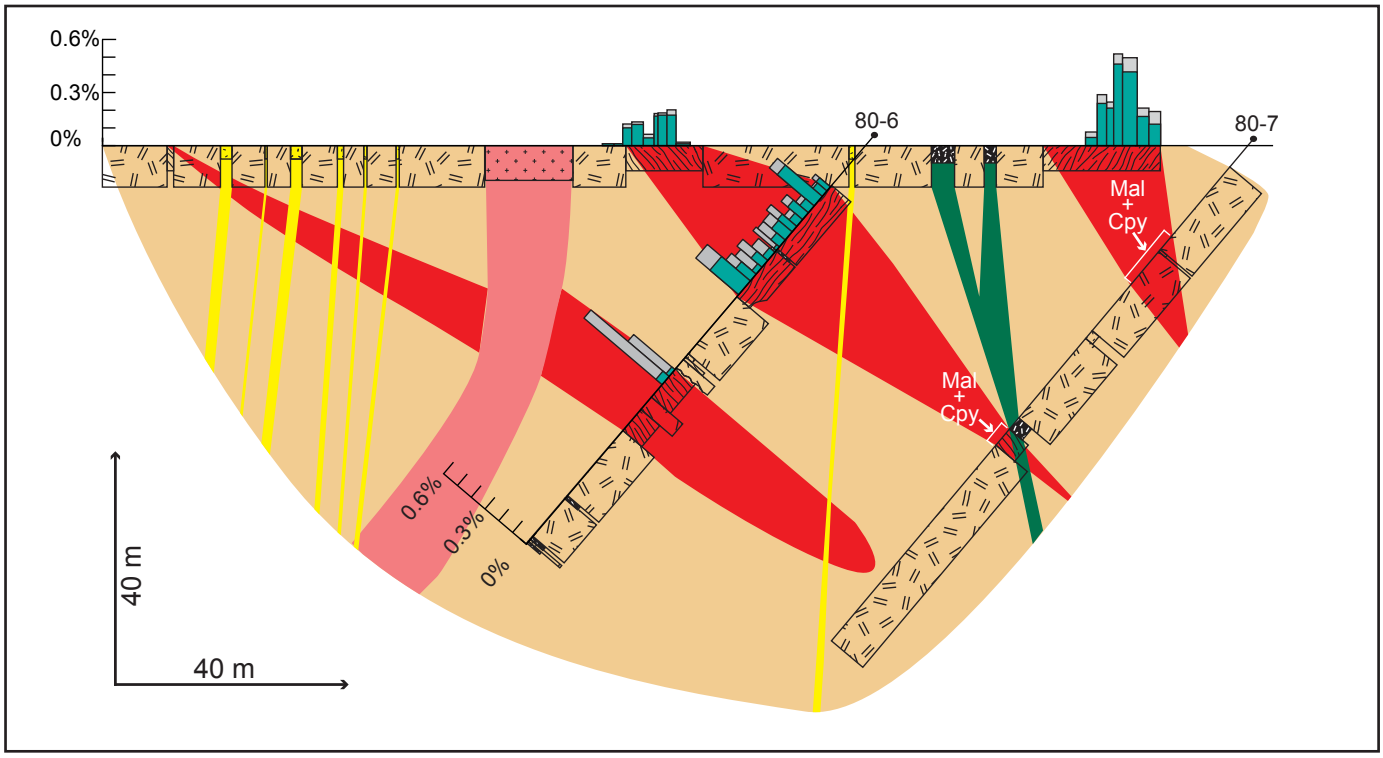

Figure 6. *Cross section of trench 800W from Zone A of the Stu occurrence, looking NW; location A-A′ shown on Figure 3. Graphic logs same as Figures 4 and 5, trench geology from 2015 re-mapping. Bar graphs show 2015 re-assayed total Cu (grey) and supergene Cu (teal) values. Diamond drill hole 80-7 was not re-assayed and mineralized zones are based on visible Cu mineralization as noted in original logs. Rock units same as Figure 3. Mal=malachite, Cpy=chalcopyrite.*

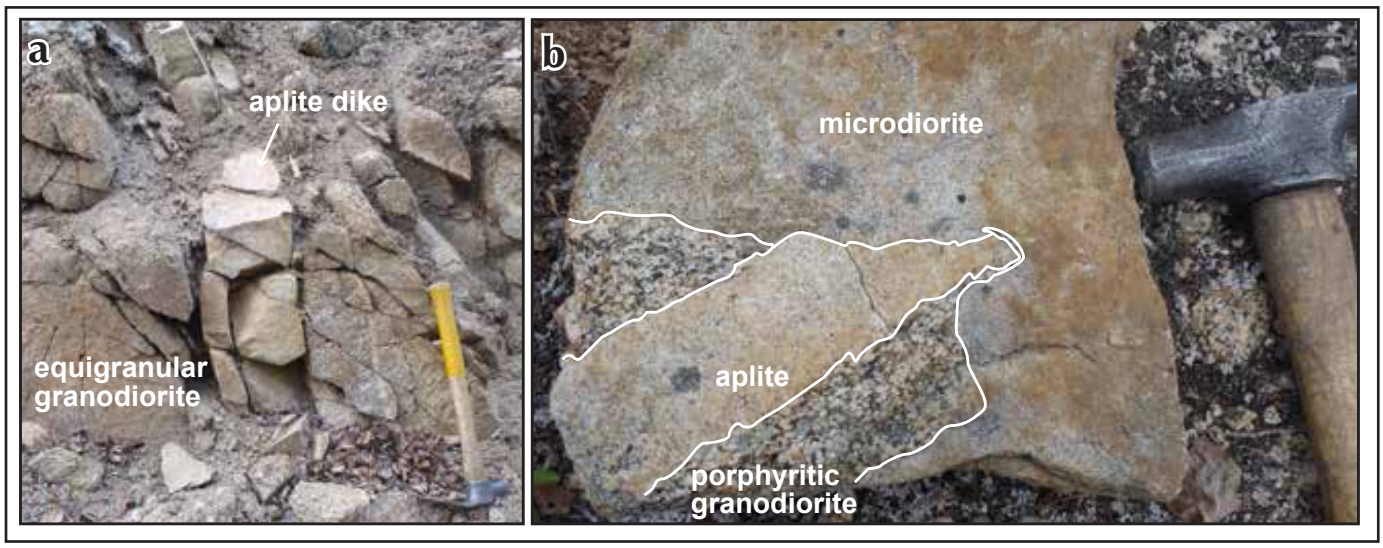

Figure 7. *Crosscutting relationship between granitoid intrusions at the Stu occurrence. (a) 20 cm thick aplite dike crosscutting equigranular granodiorite in trench 600W. (b) Three phases of granitoid intrusions in float from the B Zone. Porphyritic granodiorite cut by aplite dike, both cut by the microdiorite.*

chlorite altered with minor alteration of mafic minerals. Based on modal mineralogy, massive porphyritic rocks from the Stu property plot in, or on the lower boundary of, the granodiorite field of the Le Bas and Streckeisen (1991) classification (Fig. 8).

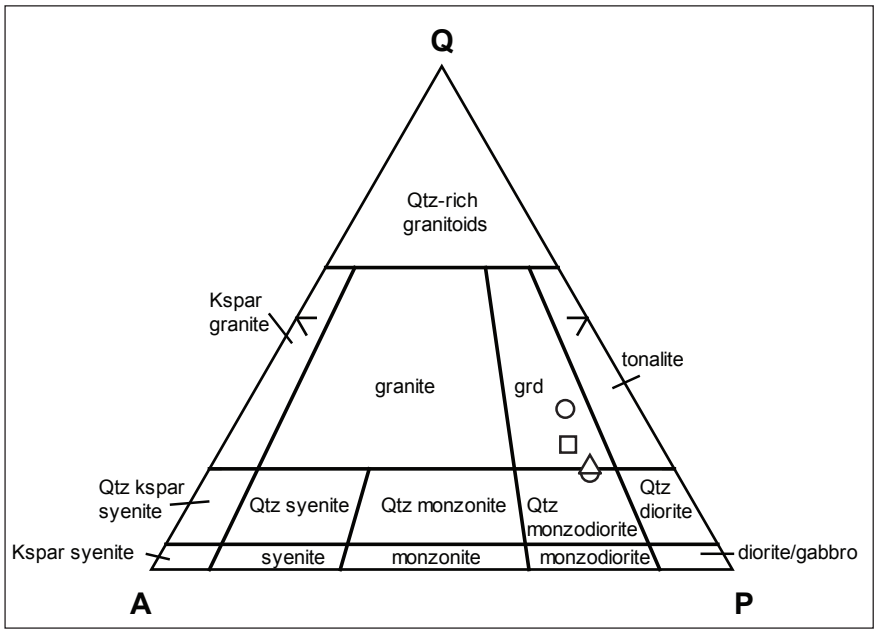

Figure 8. *Quartz-alkali feldspar-plagioclase (QAP) classification for plutonic rocks with <90% mafic mineral content (Le Bas and Streckeisen, 1991) using modal mineralogy determined by trained classification method on scans of cobaltinitrite stained slabs using ImageJ software. Qtz=quartz, Kspr=K-feldspar, grd=granodiorite. Circles=unfoliated granodiorite, square=biotite gneiss and triangle=mafic xenolith.*

Foliated and mineralized rocks also have a granodiorite composition (Fig. 8) but are equigranular and have higher biotite content than the porphyritic granodiorite. Modal mineralogy consists of quartz, plagioclase, K-feldspar, biotite, and hornblende with accessory titanite, epidote (both magmatic and deuteric), apatite and zircon (Fig. 9). The following petrographic description of foliated samples is mostly summarized from Fonseca (2008). Felsic minerals are generally anhedral to subhedral and elongate parallel to the dominant foliation. Mafic minerals typically form 5 to 15% of the rock, though locally they can reach 50%, and are subhedral to euhedral grains defining foliation. Hornblende is closely associated with biotite and locally partially biotite altered. Magnetite is the most abundant opaque mineral and forms 2 to 4% of melanocratic foliated domains as subhedral to euhedral octahedral grains that can be weakly replaced by hematite along microfissures. Hydrothermal alteration minerals are poorly developed and consist of clay and chlorite. Clay minerals alter growth zones in plagioclase and chlorite can locally partially replace biotite and hornblende along cleavage planes. Supergene copper mineralogy is

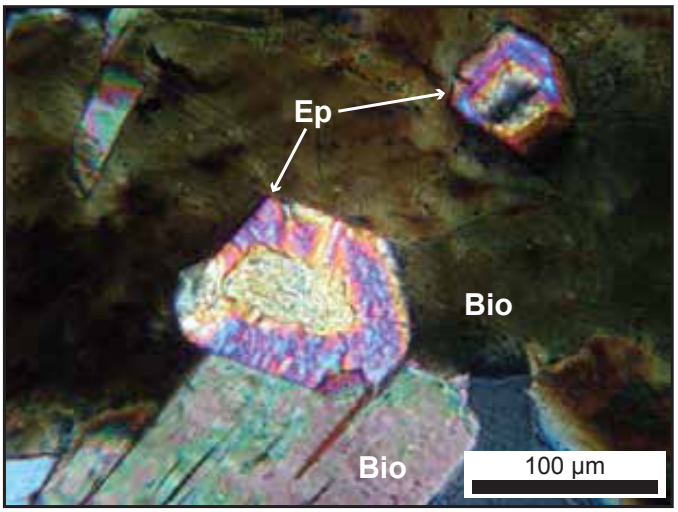

Figure 9. *Photomicrograph of euhedral magmatic epidote intergrown with euhedral magmatic biotite. Sample is a mineralized, moderately foliated granodiorite from Zone C in trench 1150E (from Fonseca, 2008). Field of view = 400 µm.*

dominantly malachite with lesser chrysocolla, azurite and tenorite. Hypogene copper mineralogy includes very fine grained chalcopyrite and bornite. In one sample, malachite and azurite replace very fine grained Cu-sulphides interpreted to have replaced primary mafic minerals; in two samples very small native gold grains (<0.5 µm) are reported. These observations suggest that primary hypogene copper mineralization occurred early in the intrusive history and, at least partly, as replacement of magmatic mafic minerals. Supergene copper is related to oxidation extent and decreases with depth (Fig. 6).

GEOCHEMISTRY

WHOLE-ROCK ANALYSES

As described above, most plutonic rocks from the Stu property (Fig. 2, 4 and 5) plot in the granodiorite field of the Le Bas and Streckeisen (1991) classification. A similarly restricted range in degree of fractionation is apparent in the whole-rock geochemical data, though there is a slight spread in the alkalinity (Fig. 10a,b). Two geochemical groups, corresponding to the quartz monzonitic and granodiorite compositions identified on the property, are separable in a variety of geochemical plots with granodiorite samples slightly less fractionated than the quartz monzonitic samples (Figs. 10 and 11). All samples are typical volcanic arc (I-type) granitoid rocks with a magnesian, calc-alkalic, metaluminous character. The one orthogneiss sample analyzed is chemically very similar to the unfoliated K-feldspar porphyritic granodiorite, and a mafic xenolith within the porphyritic granodiorite also has similar chemistry to its host, but is slightly more alkalic (Figs. 10 and 11). The aplite sample is chemically similar to the quartz monzonitic samples (Figs. 10 and 11). All whole-rock analytical results are included in appendix 2.

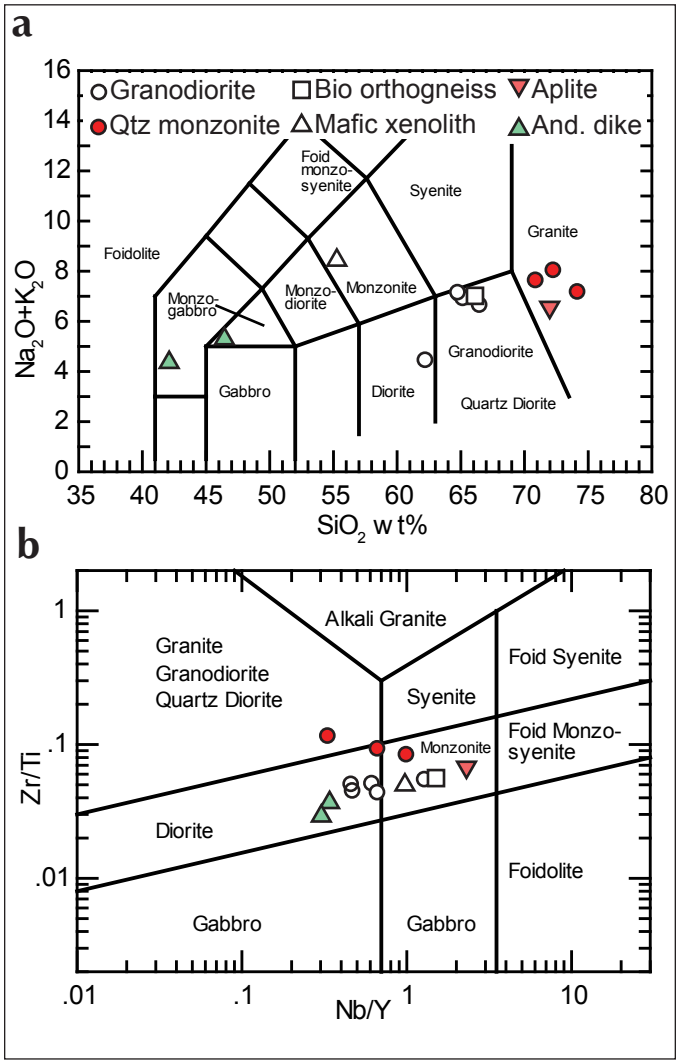

Figure 10. *Whole-rock composition plots. Symbols shown in Figure 10a. (a) Total alkali-silica plot using mobile elements (Le Bas et al., 1986), alkalinity increases on the Y-axis and degree of fractionation on the X-axis; (b) immobile element Zr/Ti vs. Nb/Y diagram of Winchester and Floyd (1977) modified by Pearce (1996), alkalinity increases on the X-axis and degree of fractionation on the Y-axis. Filled symbols are from quartz monzonitic samples on the western part of the property and have slightly more fractionated geochemistry but similar alkalinity to the granodioritic samples (hollow symbols).*

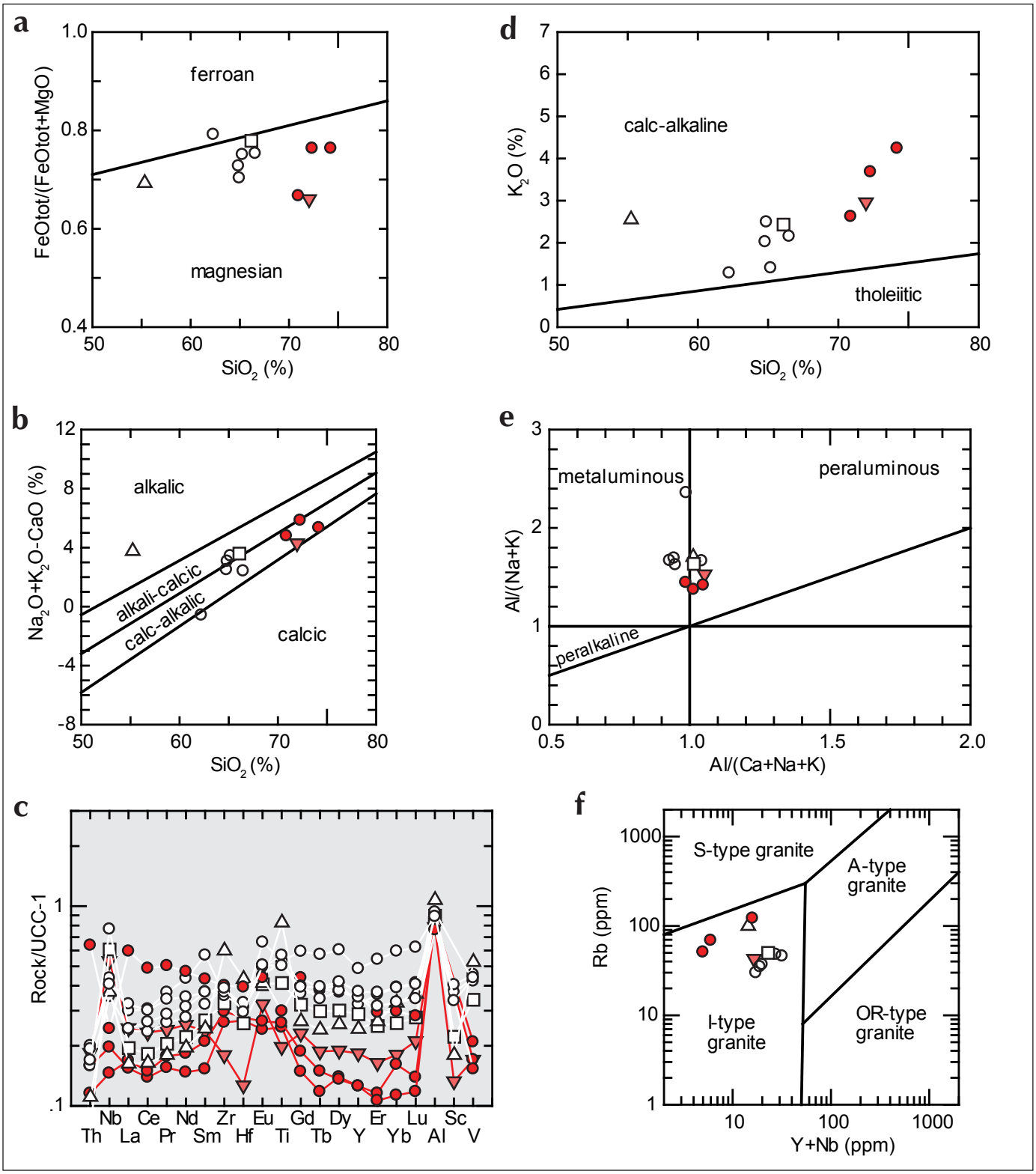

Figure 11. *Whole-rock geochemical plots. (a) Ferroan vs. magnesian granitoids (Frost and Frost, 2008); (b) modified alkali-lime index (Frost et al., 2001); (c) trace element patterns normalized to upper continental crust values of McLennan (2001); (d) Calc-alkaline vs. tholeiitic discrimination from Peccerillo and Taylor (1976); (e) alumina saturation plot of Shand (1927) from Maniar and Picolli (1989); and (f) tectonic discrimination diagram for collision zone intrusions (Harris et al., 1986). Symbols same as Figure 10a.* FeO_{tot} *=total Fe.*

ASSAY RESULTS

Samples were collected from diamond drill core and trenches. The drill core samples were collected from hole 80-6, a hole previously drilled and sampled in 1980. Most sample intervals had been split, sampled and presumably analyzed by previous operators, but the results are not available. Resampling of core left from previous work consisted of collecting composite samples, taking approximately 10 cm of remaining half-core piece every 30 cm over an average sample length of approximately 1.5 m. Trench samples were collected from trench walls as chip samples of 1 to 3 m intervals using standard exploration chip sampling methods. All assay results are included in appendix 3.

The samples collected from diamond drill hole 80-6 core were selected based on the presence of visible Cu mineralization. Sulphide and supergene Cu mineralization is generally observed in, or proximal to bodies of variably foliated granodioritic rock (Fig. 4). In the uppermost interval, from 11.58 to 35.66 m, total Cu content ranged from 0.03% to 0.34%, averaging 0.18% Cu over 24.08 m. The lowermost section is mineralized at the top of the interval, containing an average of 0.46% Cu over 3.35 m, but is unmineralized towards the bottom of the intersection (*i.e.*, <0.005% Cu). As would be expected, the ratio of supergene Cu oxide to total Cu is highest towards the top of the hole and decreases downwards. Based on this section, significant oxidation (*i.e.*, > 50% oxide to total Cu) occurs to a depth of approximately 40 m vertically from surface. Gold concentration in this hole is generally low (*i.e.*, <0.1 g/t Au), however two samples collected from the lower interval returned 0.128 and 0.272 g/t Au.

Results from trench sampling generally indicate multiple mineralized zones in each trench (Fig. 3). The ratio of Cu oxide to total Cu was >50%, indicating the majority of Cu is present as supergene Cu minerals. Gold values are generally low (*i.e.*, <0.1 g/t Au). The results of the resampling indicate three mineralized zones in trench 1150W: the eastern-most zone returned values of 0.153% total Cu and 0.083 g/t Au over 6.0 m; values from the centre include 0.124% total Cu and 0.026 g/t Au over 3.3 m; and 0.055% total Cu and 0.025 g/t Au over 14.0 m were return in the west. Trench 800W has two mineralized zones, 0.293% total Cu and 0.144 g/t Au over 12.8 m at the eastern end and 0.143% total Cu and 0.017 g/t Au over 9 m at the western end. Trench 600W does not have any significant mineralization at the eastern end, but in the west has 0.185% total Cu and 0.036 g/t Au over 27.0 m. Trench 400W has one zone containing 0.078% total Cu and 0.004 g/t Au over 6.0 m.

DISCUSSION

At least four foliated and mineralized bodies have been mapped in Zone A of the Stu property, they strike NW and dip moderately to steeply to the NE. The eastern body appears to be the largest (Fig. 3) with a minimum strike length of 200 m, a down dip extent of 80 m, and an approximate total Cu grade of 0.15%, along section 800W. Three significant intersections (>2.8 % Cu over 12.5 m or more), two within the eastern body, were drilled on the property in 1980 (Tempelman-Kluit, 1981). The best intersection to date, 3.51% Cu, 2.5 g/t Au and 18.4 g/t Ag over 13.5 m, is from hole 80-14 in Zone A (Tempelman-Kluit, 1981). In plan and cross section view, the foliated and mineralized bodies pinch and swell, appearing lensoidal in shape. Contacts between the foliated and unfoliated bodies are ambiguous but are interpreted as primarily intrusive in nature, though it is likely they were modified during deformation. Mineralized and foliated granodioritic rocks have been deformed and recrystallized to dominantly biotite orthogneiss with local biotite schist. This is similar to mineralized amphibolite, biotite schist and gneiss (Tafti and Mortensen, 2004) from Williams Creek, and foliated to gneissic banded granodiorite with mafic schlieren (Hood, 2012) from Minto.

Based on our re-assay of diamond drill core from hole 80-6, total Cu (%)/Au (ppm) ratios for Stu range from 2.2 to 10.2, supergene Cu/Au from 0.2 to 7.4, and sulphide Cu/Au from 1.3 to 9.2. Taking the two least oxidized sample intervals as representative of hypogene mineralization (Fig. 4), total Cu/Au averages 2.3 which is very similar to the ratios seen at the Minto and Carmacks Copper deposits (based on published resources of Mercer and Sagman, 2012, and Arseneau and Casselman, 2008, resepctively). The proportion of supergene Cu decreases with depth while the sulphide Cu increases (Fig. 4). Conversely Au and Ag are consistently low in shallow samples (~20 ppb and ≤1 ppm, respectively) compared to the deeper samples (200 ppb and 3 ppm, respectively). These trends suggest that Cu, Au and Ag have been mobilized during oxidation but only Cu has been re-deposited, and possibly enriched, during supergene processes.

The origin of the Minto and Carmacks Copper deposits is still debated. Early interpretations of the Minto ore bodies include metamorphosed and deformed syn-sedimentary

Cu mineralization (*e.g.*, red bed copper), or very early porphyry-style mineralization, followed by intrusion of the main unfoliated plutonic body (Pearson and Clark, 1979). Subsequent workers have utilized the presence of 'magmatic' epidote and Al-in-hornblende geobarometry to constrain the crystallization pressures of the unmineralized Granite Mountain batholith plutonic rocks to 6.1 to 6.6 kbar (equivalent to 22-24 km crustal depth; McCausland *et al.*, 2002; Tafti and Mortensen, 2004). The presence of 'magmatic' epidote in mineralized rock (*e.g.*, Fonseca, 2008) suggests models should accommodate a deeper crustal level than is typical in porphyry models (1-6 km; Seedorff *et al.*, 2005). This has been done by either, utilizing an early porphyry-style mineralization model, and invoking rapid vertical tectonic movement (Tafti and Mortensen, 2004), or using a shear-hosted magmatic-hydrothermal model whereby mineralization occurred in the mid-crustal roots of a porphyry system (Hood, 2012). Tafti and Mortensen (2004) also looked at the Carmacks Copper deposit and concluded the majority of mineralization was early porphyry-style in origin, but that supracrustal hosts (*i.e.*, metasedimentary and/or metavolcanic rocks) may have been locally important. At Carmacks Copper, others have concluded that the foliated and mineralized bodies may be rafts of mineralized volcanic rock (now amphibolite or schist; Archer, 1989; Kent *et al.*, 2014) similar to the early syn-sedimentary Cu interpretation at Minto of Pearson and Clark (1979).

The above models broadly incorporate the same key observations: 1) Cu-sulphide mineralization was emplaced early in the host rock history; 2) individual mineralized bodies have been deformed and recrystallized obscuring original characteristics; and 3) main unfoliated plutonic phases intrude, and possibly engulf the ore bodies. Observations at Stu are similar: Cu-sulphide minerals replace, at least partly, magmatic mafic minerals early in the host rock history; the host granodioritic rocks have been strongly deformed and recrystallized to the point they are now dominantly gneissic; and the primary contacts between unfoliated and foliated granodioritic rocks appear to have been intrusive in nature with the foliated and mineralized bodies surrounded by unfoliated K-feldspar porphyritic granodiorite. Limited rock exposure at the Stu, particularly of unoxidized hypogene mineralization, makes interpretation of a genetic model difficult. Based on our fieldwork, we suggest that Stu mineralization is similar to the Carmacks Cu and Minto deposits. It is primarily hosted in multiple discrete bodies of foliated granodioritic rocks striking NW and dipping to the NE. Mineralization occurs as both hypogene sulphide minerals, bornite and chalcopyrite, and supergene malachite, azurite, tenorite and chrysocolla. In terms of supergene processes, and ore body orientation, Stu is more similar to Carmacks Copper, though the overall similar character of hypogene mineralization at Carmacks Copper, Minto and Stu suggests a similar genetic model for all three. The primary difference between the three appears to be variation in the present orientation of the ore bodies which has likely influenced supergene processes.

ACKNOWLEDGMENTS

John Chapman of the Geological Survey of Canada provided whole-rock geochemical data from four samples near the Stu occurrence. Jean Pautler helped us early on with discussion and finding our way around the property. Josh Pillsbury and Don Lougheed provided superior assistance in the field. Jesse and Emily Halle and Nikolett Kovaks were gracious hosts at the Carmacks Copper camp and generously showed us their rocks.

REFERENCES

Archer, A.R., 1989. Bulk sampling and metallurgical investigations, Williams Creek Copper property, Carmacks area, Yukon Territory. Yukon Energy, Mines and Resources Assessment Report 092859.

Arseneau, G. and Cassleman, 2008. Resource Estimate of the No. 1, No. 4 and No. 7 zones Carmacks' Deposit, Yukon Territory. Internal report, Wardrop Engineering Inc., 73 p.

Colpron, M., Israel, S., Murphy, D.C., Pigage, L.C. and Moynihan, D., 2016. Yukon Bedrock Geology Map 2016. Yukon Geological Survey, Open File 2016-1, scale 1:1 000 000.

Fonseca, A., 2008. Petrographic survey of the Stu Cu-Au project, Carmacks Copper Belt, Dawson Range Yukon, Canada. Yukon Energy, Mines and Resources Assessment Report 095195.

Frost, B.R., Barnes, C.G., Collins, W.J., Arculus, R.J., Ellis, D.J. and Frost, C.D., 2001. A geochemical classification for granitic rocks. Journal of Petrology, vol. 42, p. 2033-2048.

Frost, B.R. and Frost, C.D., 2008. A geochemical classification for feldspathic igneous rocks. Journal of Petrology, vol. 49, p. 1955-1969.

Gordey, S.P. and Makepeace, A.J.(compilers), 2001. Bedrock geology, Yukon Territory. Indian & Northern Affairs Canada/Department of Indian & Northern Development: Exploration & Geological Services Division, Open File 2001-1, scale 1:1 000 000.

Harris, N.B.W., Pearce, J.A. and Tindle, A.G., 1986. Geochemical characteristics of collision-zone magmatism. *In:* Collision Tectonics, M.P. Coward and C.A. Ries (eds.), Special Publications 19, Geological Society London, p. 67-81.

Hayward, N., Miles, W. and Oneschuk, D., 2012. Detailed geophysical compilation project, Yukon Plateau, Yukon, NTS 115-I,J,K,N,O and 116A and B. Geological Survey of Canada, Open File 7279, scale 1:350 000.

Hood, S., 2012. Mid-crustal Cu-Au Mineralisation during Episodic Pluton Emplacement, Hydrothermal Fluid Flow, and Ductile Deformation at the Minto Deposit, YT, Canada. Unpublished MSc thesis, University of British Columbia, 231 p.

Joyce, N.L., Colpron, M., Allan, M.M., Sack, P.J., Crowley, J.L. and Chapman, J.B., 2016. New U-Pb zircon dates from the Aishihik batholith, southern Yukon. *In:* Yukon Exploration and Geology 2015, K.E. MacFarlane and M.G. Nordling (eds.), Yukon Geological Survey, p. 131-149.

Kent, A., Arseneau, G., Hester, M. G., Beattie, M. and Hull, J., 2014. Preliminary economic assessment of copper, gold and silver recovery at the Carmacks project, Yukon Territory, Canada. Internal report, Merit Consultants Internation Inc., 195 p.

Le Bas, M.J. and Streckeisen, A.L., 1991. The IUGS systematics of igneous rocks. Journal of the Geological Society, London, vol. 148, p. 825-833.

Logan, J.M. and Mihalynuk, M.G., 2014. Tectonic controls on Early Mesozoic paired alkaline porphyry deposit belts (Cu-Au ± Ag-Pt-Pd-Mo) within the Canadian Cordillera. Economic Geology, vol. 109, p. 827-858.

Maniar, P.D. and Picolli, P.M., 1989. Tectonic discrimination of granitoids. Geological Society of America Bulletin, vol. 101, no. 5, p. 635-643.

McCausland, P.J.A., Symons, D.T.A., Hart, C.J.R. and Blackburn, W.H., 2002. Paleomagnetism and geobarometry of the Granite Mountain batholith, Yukon: Minimal geotectonic motion of the Yukon-Tanana Terrane relative to North America. In: Yukon Exploration and Geology 2001, D.S. Emond, L.H. Weston and L.L. Lewis (eds.), Exploration and Geological Services Division, Yukon, Indian and Northern Affairs Canada, p. 163-177.

McLennan, S.M., 2001. Relationships between the trace element composition of sedimentary rocks and upper continental crust. Geochemistry, Geophysics, Geosystems, vol. 2, 24 p.

Mercer, B. and Sagman, J., 2012 Phase VI Preliminary Feasibility Report Minto Mine. Internal report, Minto Explorations Ltd., 368 p.

Nelson, J.L., Colpron, M. and Israel, S., 2013. The Cordillera of British Columbia, Yukon, and Alaska: Tectonics and metallogeny. *In:* Tectonics, Metallogeny and discovery: The North American Cordillera and similar accretionary setttings, M. Colpron, T. Bissig, B.G. Rusk and J.F. Thompson (eds.), Special Publication No. 17, Society of Economic Geologists, p. 53-109.

Pautler, J., 2009. Geological, geochemical, petrographic and compilation Assessment Report of the Stu property. Yukon Energy, Mines and Resources Assessment Report 095195.

Pearce, J.A., 1996. A user's guide to basalt discrimination diagrams. Trace element geochemistry of volcanic rocks. *In*: Wyman, D.A. (ed.), Geological Association of Canada - Mineral Deposits Division, p. 79-113.

Pearson, W.N. and Clark, A.H., 1979. The Minto copper deposit, Yukon Territory; a metamorphosed orebody in the Yukon crystalline terrane. Economic Geology, vol. 74, p. 1577-1599.

Peccerillo, A. and Taylor, S.R., 1976. Geochemistry of eocene calc-alkaline volcanic rocks from the Kastamonu area, Northern Turkey. Contributions to Mineralogy and Petrology, vol. 58, p. 63-81.

Sánchez, M.G., Allan, M.M., Hart, C.J.R. and Mortensen, J.K., 2014. Extracting ore-deposit-controlling structures from aeromagnetic, gravimetric, topographic, and regional geologic data in western Yukon and eastern Alaska. Interpretation, vol. 2, p. SJ75-SJ102.

Seedorff, E., Dilles, J.H., Proffett, J.M., Einaudi, M.T., Zurcher, L., Stavast, W.J.A., Johnson, D.A. and Barton, M.D., 2005. Porphyry deposits: Characteristics and origin of hypogene features. *In:* Economic Geology: One Hundredth Anniversary Volume, J.W. Hedenquist, J.F.H. Thompson, R.J. Goldfarb and J.P. Richards (eds.), Society of Economic Geologists, p. 251-298.

Shand, S.J., 1927. Eruptive rocks: Their genesis, composition, classification, and their relation to ore-deposits, with a chapter on meteorites. T. Murby & Co., London, 360 p.

Tafti, R. and Mortensen, J.K., 2004. Early Jurassic porphyry(?) copper (-gold) deposits at Minto and Williams Creek, Carmacks Copper Belt, western Yukon. *In:* Yukon Exploration and Geology 2003, D.S. Emond and L.L. Lewis (eds.), Yukon Geological Survey, p. 289-303.

Tempelman-Kluit, D.J., 1981. Description of the Stu property. *In:* Yukon Geology and Exploration 1979-80. Department of Indian and Northern Affairs, Geology Section, Whitehorse, Yukon, p. 262-263.

Tempelman-Kluit, D.J., 1984. Geology of Laberge (105E) and Carmacks (115I) map areas, Yukon. Geological Survey of Canada, Open File 1101.

Watson, K.W. and Joy, R.J., 1977. Geological, geochemical and geophysical report on the Stu claim group, Hoochekoo Creek area. United Keno Hill Mines Ltd., Yukon Energy, Mines and Resources Assessment Report 090248.

Winchester, J.A., Floyd, P.A., 1977. Geochemical discrimination of different magma series and their differentiation products using immobile elements. Chemical Geology 20, p. 325-343.

Woodsworth, G.J., Anderson, R.G. and Armstrong, R.L., 1991. Plutonic Regimes, Chapter 15. *In*: Geology of the Cordilleran Orogen in Canada, H. Gabrielse and C.J. Yorath (eds.), Geological Survey of Canada, Geology of Canada, no. 4, p. 491-531; *also Geological Society of America, The Geology of North America, vol. G-2*.

Yukon Geological Survey, 2015. Yukon Digital Bedrock Geology. <http://www.geology.gov.yk.ca/update_yukon_bedrock_geology_map.html> [accessed November 20, 2015].

Zen, E. and Hammarstrom, J.M., 1984. Magmatic epidote and its petrologic significance. Geology, vol. 12, p. 515-518.

APPENDICES

The three appendices for this paper are only available digitally. The 3D geologic model in Appendix 1 requires a free software viewer, see details below. Appendices 2 and 3 are separate tabs within one Microsoft Excel spreadsheet.

Appendix 1. A simplified 3D geological model for the Zone A occurrence on the Stu property is included in this digital appendix. The model was created from a series of sections (e.g., Fig. 6), using geological information from the three diamond drill holes and trenches logged in this study and from digitized historic drill sections for the remaining holes in Zone A. The model includes drill hole and trench geological data, assay data collected from this study, and historically reported drill intercepts. The model can be viewed and manipulated using Geosoft Montaj Viewer; free software available for download from the Geosoft website (http://www.geosoft.com/support/downloads/viewers/oasis-montaj-viewer). The Geosoft website provides directions for downloading and configuring the freeware. Once the file containing the model (STU 3D view.gpf) is open in Geosoft Montaj Viewer, the user can manipulated the model in 3D space by selecting the 3D tab in the top menu bar then selecting the rotation, zoom or pan options in the 3D window menu. Geologic units in the model same as Fig. 3.

Appendix 2. Whole-rock geochemical analyses. Whole-rock analysis of 13 samples was conducted at Activation Laboratories Ltd., Ancaster, Ontario, using the 4Lithoresearch analytical package, a lithium metaborate/tetraborate fusion followed by analysis using Inductively Coupled Plasma Mass Spectrometry (ICPMS). For major elements, the quality of these data meet or exceeds fusion x-ray fluorescence data. For trace elements, the fusion process provides total dissolution of refractory minerals such as zircon, sphene and monazite, and gives accurate rare earth and high field strength element data. Using this analytical package, detection limits for major elements are 0.001% to 0.01% and trace elements are typically better than 1 ppm.

Appendix 3. Assay data, including sulphide and supergene Cu analyses. Geochemical analyses were conducted by Bureau Veritas Mineral Laboratories Ltd. using standard preparation and analytical techniques. Each sample was

prepared by crushing then pulverizing to 200 mesh. The 200 mesh pulps were analyzed for 41 elements by 4-acid digestion and Inductively Coupled Plasma Emission and Mass Spectrometry (ICPES/ICPMS) depending on the best technique for each element. Gold was analyzed by fire-assay fusion with an atomic absorption analysis (FA-AAS) and supergene Cu was analyzed by weak sulphuric acid digestion (5% H_2SO_4) followed by an ICPMS analysis.